Absolute Localization via DSRC Signal Strength

Samir Al-Stouhi
Honda R&D Americas Inc.
Southfield, MI
salstouhi@hra.com

Radovan Miucic
Honda R&D Americas Inc.
Southfield, MI
rmiucic@oh.hra.com

***Abstract*—Lane-level localization is the basis for successful deployment of Intelligent Transportation Systems. Global Navigation Satellite System (GNSS) can provide lane-level position in open (non-obstructed) environments. Inertial and relative ranging sensors can maintain position estimate after GNSS signal loss while slowly drifting. A new area of research aims for a collaborative approach to localization where one vehicle can leverage the localization information from other vehicles. A Dedicated Short Range Communication (DSRC) message has all surrounding vehicles' location data and complementing this message is its Received Signal Strength (RSS). The RSS from a DSRC message can be used as a relative ranging sensor to a vehicle with known location allowing for recovery of one's own absolute position. In this paper, we demonstrate a successful implementation of absolute localization via ranging from RSS using an extensive dataset collected from 30 DSRC equipped vehicles. First, we analyze the obstacles to localization via RSS and propose a set of methods for absolute localization from the RSS of DSRC messages. We than integrate our methods with the prior from vehicle dynamics and demonstrate that a practical absolute localization can be recovered from RSS. We finally demonstrate our algorithms' absolute positioning potential for both static and dynamic environments and present concepts for further improvements.**

I. Introduction

Affordable lane-level localization is a cornerstone for the successful deployment of DSRC applications. An urban canyon environment is the most challenging localization environment as it deprives the user of line of sight to the GNSS satellites. In the absence of GNSS, there are no economical absolute localization techniques and thus current approaches to localization apply relative localization (from last GNSS position) via dead reckoning. High definition maps are one economical method for absolute localization but require a relatively precise location to minimize the map search space.
An urban canyon is a mixed environment where neighboring vehicles have different localization accuracy variances subject to their route history (and that route's skyline obstruction), the accuracy of their positioning equipment, and other stochastic events. In this environment, the dense availability of DSRC equipped vehicles presents an opportunity to overcome GNSS limitation as each vehicle can posses the location data (transmitted over DSRC) of all neighboring vehicles and in turn use this data for self localization. All DSRC equipped vehicles are required to send a BSM, that includes 3D location, at an expected minimum rate of 1HZ. With the contents of a BSM, a receiver only needs a relative ranging sensor and can in return obtain an absolute fix of its own location. Allowing a vehicle to match its own localization solution to that of the surrounding vehicle with the most accurate solution provides a new method for absolute localization. Vehicles can also propagate higher localization confidence in the DSRC VANET.
In this paper, we propose multiple algorithms to acquire an absolute position using vehicle dynamics and the RSS and contents of received BSMs. Unlike other relative ranging sensors, such as radar or camera, the BSM's RSS can be modeled to estimate range to objects with known absolute position thus providing an absolute absolute position. We discuss obstacles to RSS localization and validate the performance of our algorithms with multiple experiments using $\approx$ 280,000 measurements and $\approx$ 28,000 discrete time steps in a test trial involving 200 (30 logging) DSRC transmitting vehicles. We present, to our knowledge, the first accurate DSRC localization algorithms with a large scale trial.

II. Related Works

An overview of cooperative positioning using DSRC is presented in [1]. Authors in [2] and [3] analyzed RSS, Time of Arrival (TOA), Time Difference of Arrival (TDOA) and Doppler shift [4] methods for ranging and concluded that a possible combination of all of these approaches makes the best strategy for position estimation. In a previous study [5], a DSRC RSS model with least-squares minimization was developed with the conclusion that ranging from RSS was too error prone and not feasible for localization. Authors in [6] proposed a vehicle localization system that used a Kalman filter integrating GNSS positions coupled with RSS ranging, vehicle dynamics, and road constraints. A simulation in [7] integrates GNSS, RFID, DSRC and dead reckoning for localization.
Cooperative positioning has been proposed in the realm of vehicles sharing ranging information. Data transfer bandwidth is a main issue in developing such systems. Methods including the work in [8] use DSRC as a transport mechanism to exchange GNSS pseudorange information among neighboring vehicles. The authors in [9] proposed multi-vehicle cooperative localization with a Probability Hypothesis Density filter to improve the efficiency of data transfer.
Wireless vehicular localization also use Ultra Wide Band (UWB) communication ranging [10]. UWB systems are well suited for localization because their wide transmission bandwidths provide more accurate ranging and obstacle penetration capabilities. However, UWB is not currently considered an option for transportation safety systems.
Finally, absolute localization can be combined with relative ranging sensors (such as cameras or radars) for further refinement if ambiguities in constructing a map (and absolute location) of neighboring vehicles can be resolved. The authors in [11] used information from neighbor vehicles in binary form using a vision-based sensor system to associate each vehicles location with its identification.

III. Range Estimation from RSS

A BSM includes, amongst other data, vehicle's status, transmission power, and position. A receiver measuring the RSS can model range between transmitter and receiver. Once range is estimated from RSS, the reference location received from the transmitting vehicles can be used by the receiver to localize itself. In this section, we describe how RSS data was collected and modeled to estimate range.

A. Experiment Setup

The dataset was collected by the Vehicle Safety Communication 3 (VSC3) consortium with 200 DSRC equipped vehicles. Data was collected at the Transportation Research Center in Ohio [12]. Figure 1 presents an overview of the test setup where the movement patterns mimicked an intersection and 8 large trailers were parked at the intersection to block signals and mimic buildings. While all 200 vehicles were transmitting, only data from 30 unique vehicles was collected and used in this paper.
The reference vehicle, localized in this paper, started from the center of the intersection and moved toward the bottom right of Figure 1 before going back to its starting position. This procedure was repeated 5 times for a travel distance of $\approx 6km$ while taking 27,950 discrete time steps and collecting 278,634 measurements.

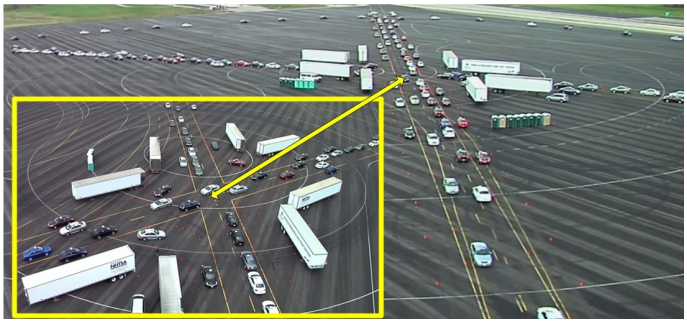

Fig. 1: Illustration of the intersection setup

B. Range Estimate from DSRC Signal Strength

The simplest model of the signal strength propagation over distance is the Free Space Propagation model.

$$P_r(R) = \frac{P_t G_t G_t}{L}(\frac{\lambda}{4\pi R})^2 \tag{1}$$

where $P_r(R)$ is the received power (in W) of the separation distance R (in m), P_t is the transmitted power (in W), G_t is the transmitter antenna gain (unit less), G_r is the receiver antenna gain (unit less), λ is the wavelength (in m), and L is the system loss factor ($\geq$1 and unit less) accounting for losses other than propagation [13].An improved propagation model is the combined path loss and shadowing model [14] where:

$$\frac{P_r}{P_t}(dB) = 10\log_{10} N - 10\gamma \log_{10} \frac{R}{R_0} + \psi_{dB} \tag{2}$$

$$N(dB) = -20\log_{10}(4\pi d_0/\lambda) \tag{3}$$

Where N is a unit-less constant which depends on the antenna characteristics and the average channel attenuation, R_0 is a reference distance for the antenna far-field, γ is the path loss exponent, and ψ_{dB} is a Gauss-distributed random variable with zero mean and variance $\sigma^2_{\psi_{dB}}$. Solving for R in Equation 2 provides a mapping [15] from signal strength to estimated distance as:

$$R = R_0 10^{(\frac{10\log_{10} N - P_r/P_t + \psi_{dB}}{10\gamma})} \tag{4}$$

Due to scattering, Equation 4 is generally valid for distances that are a few car-lengths away. Simple models like the the model in Equation 4 capture the essence of signal propagation, however such model provide only an approximations to the real channel which behaves often time differently.

C. Range Variance from DSRC Signal Strength

1) Range Variance: The authors in [2] use the path loss model in [16] to calculate the Cramer-Rao Lower Bound (CRLB) for the variance of RSS-based range R, where the CRLB for variance σ_R was calculated as:

$$\sigma_R^2 = \frac{\sigma^2 (R \ln(R))^2}{m^2 + \sigma^2} \tag{5}$$

Where m is the mean and σ is the variance of the normally-distributed path loss model in [16]. Equation 5 shows that, for any given path lass model, the range variance increases exponentially with the estimated range.

2) Directional Variance: In our previous study [17], an analyzed DSRC antenna setup and we present our results in Figure 2 to demonstrate that DSRC antennas also suffer from directional variation. In this paper, we used antenna setup "d".

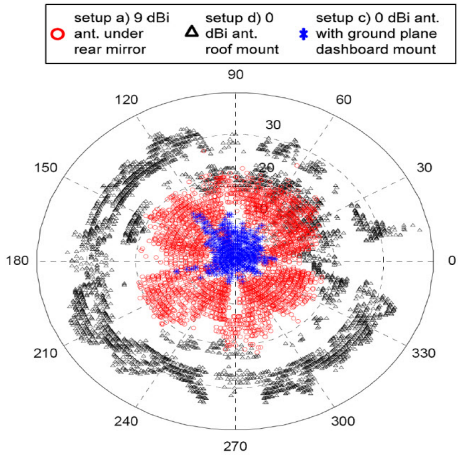

Fig. 2: RSS vs incident angle for different antenna setups

D. RSS Modeling for Range Estimate and Variance

Analysis of RSS from the dataset described in section III-A shows that the models described in section III-B do provide realistic match to our real world experiment. A plot showing

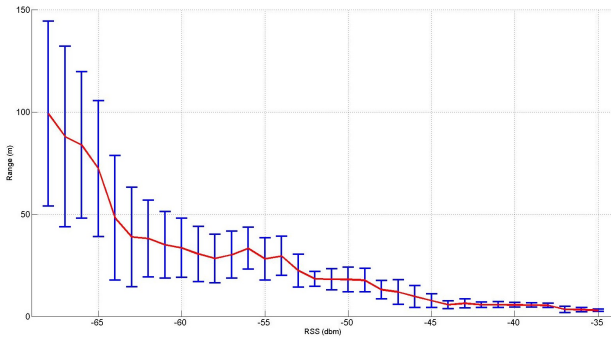

Fig. 3: RSS vs Range (Mean and Standard Deviation)

the relationship between RSS and range for the dataset is presented in Figure 3. The plot in Figure 3 demonstrates that while there is a, non-linear, correlation between RSS and range, this correlation is prone to errors. The high degree of error variances is an expected outcome of the noise in our test environment where there are both moving obstacles (vehicles) and static ones (trailers). At frequencies of 5.9GHz, the ground acts as a reflector acting in either a constructive or destructive manner depending on the distance between the transmitter and the receiver. This results in error that is also combined with multi-path arising from signals being reflected or diffracted [18]. Finally, Figure 3 demonstrates that both range and variance are correlated to RSS. To map RSS to range, we used piece-wise linear interpolation to model the discrete (integer) values for the RSS included in received BSM messages and accordingly we used the model to associate range and variance.

IV. Direct Localization

In this section, we propose methods to derive a position using only the RSS model.

A. Problem Definition

We define the 2-D positioning function at time t as the non-linear function r^t with position P^t and 2-D local coordinates, $\left(P_x^t, P_y^t\right)$, minimizing the residual:

$$r^t\left(P_x^t, P_y^t\right) = \left(Z^t - \hat{Z^t}\right) \tag{6}$$

Where the range measurement set Z^t is derived from the RSS model and comprise set of all m measurements where R_i^t is the i^{th} measurement as:

$$Z^t = \left[\begin{array}{cccc} R_1^t & \dots & R_i^t & \dots & R_m^t \end{array}\right] \tag{7}$$

The estimated range measurements $\hat{Z_i^t}$ is derived as the Euclidean distance between the i^{th} vehicle position (x_i^t, y_i^t) and the estimated receiver position $\left(P_x^t, P_y^t\right)$ as:

$$\hat{Z_i^t} = \sqrt{\left(P_x^t - x_i^t\right)^2 + \left(P_y^t - y_i^t\right)^2} \tag{8}$$

We minimized this non-linear function as a weighted least squares problem with m^t measurements as:

$$\min_{P_x^t, P_y^t} \sum_i^{m^t} w_i^t \left\| r_i^t\left(P_x^t, P_y^t\right)\right\| \tag{9}$$

Where the weight w_i^t was set to the RSS model's variance as:

$$W^t = \left[\begin{array}{ccc} w_1^t & \cdots & 0 \\ \vdots & \ddots & \vdots \\ 0 & \cdots & w_m^t \end{array}\right] = \left[\begin{array}{ccc} \sigma_1^t & \cdots & 0 \\ \vdots & \ddots & \vdots \\ 0 & \cdots & \sigma_m^t \end{array}\right] \tag{10}$$

This non-linear weighted least squares problem is first linearized via Taylor Series Expansion and then solved with the "Gauss-Newton" minimization algorithm where the linearized update is solved via least squares weighted by the matrix W. The Jacobian matrix of the update mechanism was calculated to be the unit vector as:

$$H^t = \left[\begin{array}{cc} \frac{\left(P_x^t - x_1^t\right)}{\hat{Z_1^t}} & \frac{\left(P_y^t - y_1^t\right)}{\hat{Z_1^t}} \\ \vdots & \vdots \\ \frac{\left(P_x^t - x_m^t\right)}{\hat{Z_m^t}} & \frac{\left(P_y^t - y_m^t\right)}{\hat{Z_m^t}} \end{array}\right] \tag{11}$$

This algorithm starts with the initial guess $P_{x,y}^0$ and updates the position estimate $P_{x,y}^{t+1}$ as:

$$P_{x,y}^{t+1} = P_{x,y}^t + \left[\left(H^t\right)^T W H^t\right]^{-1}\left(H^t\right)^T W r_{x,y}^t \tag{12}$$

Until the residual change converges $(\varepsilon \approx 0)$ as:

$$\left\| r_{x,y}^{t+1} - r_{x,y}^t \right\| < \varepsilon \tag{13}$$

V. Integrated Localization

A. Kalman Filter with Range Measurements

The knowledge of vehicle dynamics can improve localization as it provides a prior that can estimate the validity of the range measurements.

1) Prediction Update: The predicted position of the vehicle at time t is is updated using the velocity V^t measurement extracted from the vehicle's odometry as published on the vehicles internal bus and transmitted as part of the outgoing BSM message. In our experiments, the absolute heading, θ^t, was extracted from GNSS heading. In actual implementation heading could be derived from a magnetometer and maintained with differential wheel speed or an Inertial Measurement Unit (IMU). Since the outgoing BSM message has a variable transmission rate, the message's time-stamps were integrated into the discrete transition model f with the variable sampling interval dt as:

$$P^t = f\left(P^{t-1}\right) = \left[\begin{array}{c} P_x^{t-1} \\ P_y^{t-1} \end{array}\right] + \left[\begin{array}{c} V^t \cos\left(\theta^t\right) dt \\ V^t \sin\left(\theta^t\right) dt \end{array}\right] \tag{14}$$

The prediction variance S^t is updated as:

$$S^t = F\left(P^t\right) S^{t-1}\left[F\left(P^t\right)\right]^T + Q^t = S^{t-1} + Q^t \tag{15}$$

Where it is updated with the vehicle model noise Q^t using the position Jacobian matrix $\left(F\left(p^t\right) = I\right)$.

2) Measurement Update: The observation matrix was defined in the previous section for the "Gauss-Newton" minimization in Equation 7 while Equation 11 is its Jacobian matrix. The covariance of the measurement N is simply the range covariance which was defined as the weight matrix in Equation 10 while the measurement prediction can also be calculated using Equation 8 from the previous section using the position p^t in Equation 14. Finally, the innovation v^t can simply be calculated using the residual function in Equation 6. The innovation covariance, Σ_i^t, with the measurement noise $N^t = W^t$ would thus be updated as:

$$\Sigma_i^t = H_i^t S^t H_i^t + N_i^t = H_i^t S^t H_i^t + W_i^t \tag{16}$$

With the the innovation and its covariance calculated, a validation gate was derived to validate the correspondence between predictions and observations. Considering the inherently high dispersion index of the RSS model and the complex stochastic nature of different measurement environments, we propose a validation gate that takes the environment information into account.

In our model, we applied batch processing of received RSS data. We processed received RSS measurements every transmission. When the vehicle moved at higher speeds, the error increased due to the non-synchronous reception rate and thus we set a speed-dependent gate threshold as:

$$\left(v_i^t\right)^2 \left(\Sigma_i^t\right)^{-1} < \alpha \frac{speed + \sigma}{speed^\beta + \sigma} \tag{17}$$

Where $(v_i^t)^2 (\Sigma_i^t)^{-1}$ is the Mahalanobis distance, $\sigma \approx 0$, α is a gate threshold, and β controls the gate's threshold decay rate w.r.t speed.

With the measurements within the validation gate, we re-update the measurement predictions and covariance with the measurements that passed the gate threshold and finally update the position and variance via the Kalman gain K as:

$$\begin{aligned} K &= P^t H^t (\Sigma_i^t)^{-1} \\ P^t &= P^t + K v_i^t \\ S^t &= (I - K^t H^t)\, S^t \end{aligned} \tag{18}$$

Using a Kalman filter with range measurements has the advantage that it can improve localization via single observations and is computationally efficient. However, it uses range measurements from an RSS model that has high variance and no directional measurements.

For a better estimate, we propose a second method where the range measurement from Equation 7 would be replaced with the "Gauss-Newton" weighted least squares localization derived in Equation 12. This method should be less susceptible to noise and since it uses weighted measurements, would minimize a weighted error where the measurements with lower variance have more importance.

VI. Experiment Setup

In this section we describe the algorithm setup for our experiments. The following list describes the algorithm setup.

- Range: Raw range from the RSS model.
- GN-LS: Gauss-Newton with least squares $(W = I)$.
- GN-WLS: Gauss-Newton with weighted least squares.
- Med-Short/Long: GN-WLS with a running median filter of length (1 second) for short and length (10 seconds) for long.
- KL-R: Kalman Filter with raw range measurements from the RSS model. The initial location is set to the position of the nearest vehicle.
- KL-WLS: Kalman Filter where range measurements are calculated using GN-WLS. The initial location is set using GN-WLS.
- GNSS (Static Location): While the vehicle was static, we used a continuously running median filter to get an estimate of the error inherit to GNSS for better isolation of the source of localization error.

The median of GNSS (Static Location) was used as ground truth when the vehicle was static. When the vehicle was dynamic, GNSS raw measurements was used as ground truth.

VII. Results for Direct Localization

In this section, we present the positioning results for our direct algorithms.

A. Static Localization Error

Figure 4 shows the Cumulative Distribution Function (CDF) for localization of a static vehicle using the direct methods. The results demonstrate that processing of range estimates with GS-WLS and median filtering can provide significantly improved estimates over raw range measurements. A long median filter integrated with GS-WLS provides the best static position estimates.

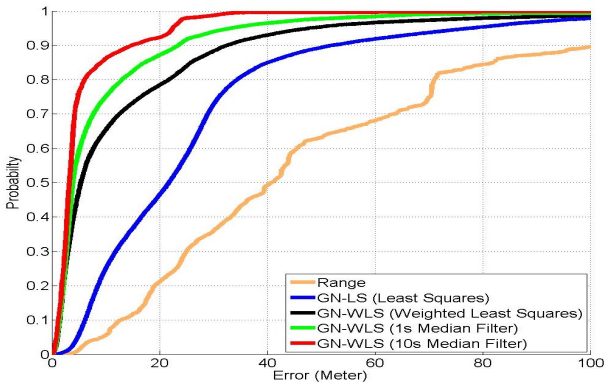

Fig. 4: CDF for static localization via direct methods

B. Mapping of Dynamic Localization

In Figure 5, we plot the position estimates of our vehicle where we overlaid GS-WLS with median filtering and ground truth. The results demonstrate that while a longer median filter provides better static results, it doesn't integrate well when the vehicle is moving. Alternatively, a short median filter (or non) reacts faster to vehicle movement while experiencing a high level of error and noise.

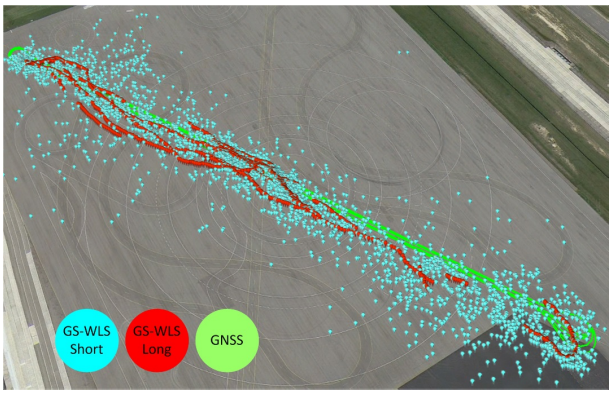

Fig. 5: Position estimate with GN-WLS with median filtering

VIII. Analysis of Integrated Localization

In this section, we present the positioning results for our integrated algorithms

A. Static Localization Error

This section will compare our algorithms' errors for static localization. In Figure 6 we plot the CDF of the difference between the median filtered GNSS (ground truth) and our integrated methods. We also plot the error for the raw GNSS measurements to show the inherit variance in GNSS. The CDF demonstrates that our integrated methods' static localization error is significantly better than direct localization. In our experiments, the localization error never exceeded 5m for KL-WLS.

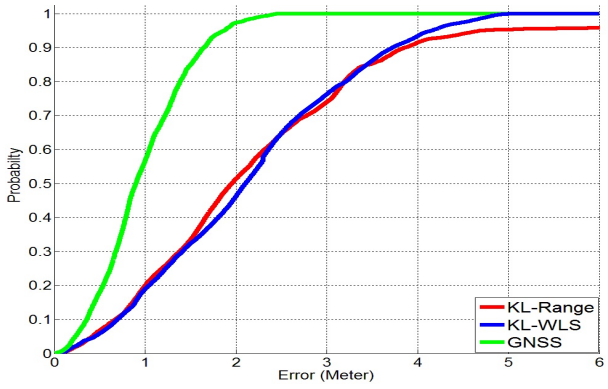

Fig. 6: CDF for static localization via Integrated methods

B. Mapping of Static Localization

To visualize static localization, we present our KL-WLS results overlaid on a map with GNSS from 6 continuous runs. Figure 7 shows the static position estimates at the intersection that was surrounded by trailers blocking DSRC signals during data collection. The map shows that GS-WLS position estimates have more variance than GNSS but are still confined within a small area.

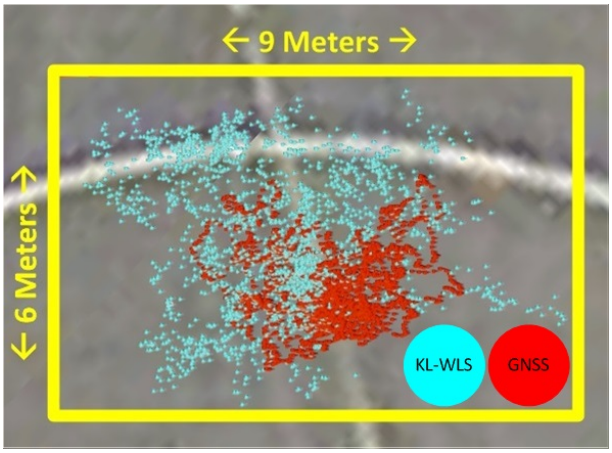

Fig. 7: Static Localization with KL-WLS

C. Mapping of Dynamic Localization

To visualize the overall localization accuracy, Figure 8 presents a map with our KL-WLS results and raw GNSS. The figure demonstrates that our localization position continuously match the GNSS position.

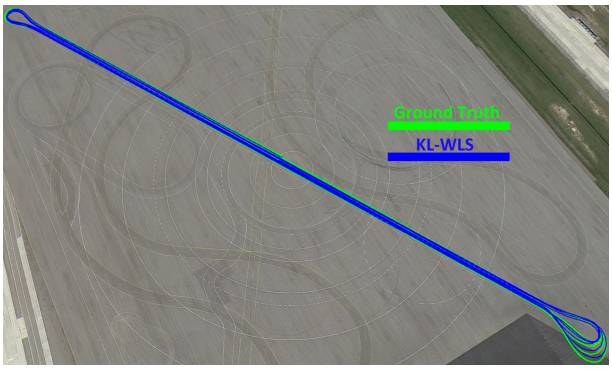

Fig. 8: Dynamic Localization with KL-WLS

D. Comparison with Dead-Reckoning

To validate the performance of GS-WLS localization, we added directional drift. We added speed ($(\mu = 0.5, \sigma = \pm 0.5) m/s$) and heading (-1%) to our vehicle model and presented the results in Figure 9. The figure shows our method (KL-WLS) and also the same method with only the vehicle model update (no RSS measurement update) depicting a standard dead-reckoning system. The initial position for both methods was initialized using GS-WLS.The figure demonstrates that after all 6 stops, GS-WLS converged to the correct absolute position while dead reckoning continued drifting many kilometers away.

IX. Tabulated Results

An overview of our DSRC localization results is presented in Table I. The following conclusions can be derived from Table I:

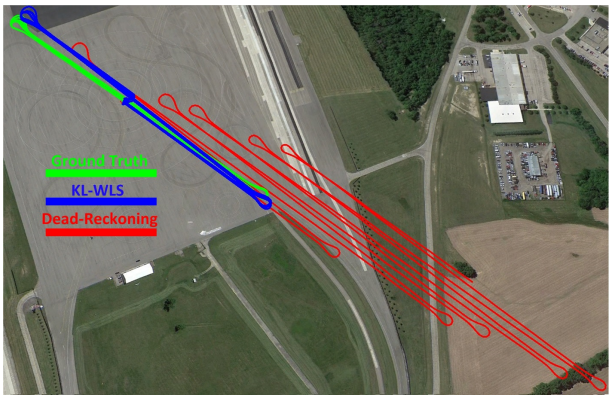

Fig. 9: KL-WLS localization vs standard dead reckoning

- Range from the RSS model has a very high error rate while GS-LS is not an effective localization method.
- Adding weights to least-squares minimization, associated with filtering improve localization.
- An algorithm with prior from vehicle model can produce reliable position estimates and serve as a basis for other sensors (vision, map-matching) for lane-level localization in the absence of GNSS.

TABLE I: Localization accuracy results

Environment	Static		Dynamic	
CDF	$\mu+\sigma$	$\mu+2\sigma$	$\mu+\sigma$	$\mu+2\sigma$
Range	45.4	220.2	57.4	220.2
GN-LS	25.1	113.7	27.9	151.8
GN-WLS	5.8	99.9	10.7	151.5
GN-WLS-Med-1s	4.3	54.4	6.7	110.7
GN-WLS-Med-10s	3.7	25.0	4.1	34.8
KL-Range	2.6	8.1	2.5	8.0
KL-GN-WLS	2.6	4.8	2.5	5.7
GNSS	1.2	2.4	-	-

X. Extensions and Discussion

In this work, we presented a set of methods to demonstrate the feasibility of localization in an open sky environment. In this section, we propose possible research directions for more robust DSRC localization.

- **Algorithmic Improvements:** Median filtering revealed promising results for static localization and a straightforward extension would be to integrate a speed controlled dynamic length median filter with GS-WLS.
- **Signal Processing Improvements:** The starting point for our localization accuracy is the RSS variance derived from our single antenna performance. Since DSRC deployment might require multiple antennas, the performance could be improved by minimizing both directional and absolute variance. With spatial filtering and antenna diversity, the variance could be further reduced.
- **Urban environment localization:** A larger scale study with more complex urban environments is required for a better interpretation of DSRC localization potential.

XI. Conclusion

In this paper, we used an extensive dataset of field DSRC data to demonstrate that the Received Signal Strength (RSS) within a DSRC Basic Safety Message (BSM) can be modeled to recover the absolute position of a vehicle. We created an RSS mode to recover range between vehicles and associated variance. The model was first used for localization using a set a methods for localization. Using only the RSS model's estimated range and variance, integrated with median filtering, provided inaccurate positioning. Two Kalman Filter methods were than implemented to integrate either raw range measurements or a Gauss-Newton weighted least-squares measurements with a prior from the vehicle model to output an absolute position. We demonstrated the validity of our localization method and demonstrated that DSRC localization can serve as basis for absolute positioning in the absence of GNSS. Finally, we presented a set of possible extensions to improve performance and motivate for further research.

References

[1] R. Aquino-Santos, R. Aquino-Santos, A. Edwards, and V. Rangel-Licea, *Wireless Technologies in Vehicular Ad Hoc Networks: Present and Future Challenges*, 1st ed. Hershey, PA, USA: IGI Global, 2012.

[2] N. Alam, A. T. Balaei, and A. G. Dempster, "Range and range-rate measurements using DSRC: facts and challenges," in *in IGNSS Symposium 2009, Surfers Paradise,Australia*, 2009.

[3] N. Alam, "Vehicular positioning enhancement using DSRC," Ph.D. dissertation, University of New South Wales, New South Wales, 2012.

[4] N. Alam, A. Tabatabaei Balaei, and A. Dempster, "A DSRC doppler-based cooperative positioning enhancement for vehicular networks with GPS availability," *Vehicular Technology, IEEE Transactions on*, vol. 60, no. 9, pp. 4462–4470, Nov 2011.

[5] R. Miucic, Z. Popovic, and S. Bai, "Position estimate assisted by DSRC for outdoor wireless environments," *SAE 2014 World Congress*, 2014.

[6] R. Parker and S. Valaee, "Vehicular node localization using received-signal-strength indicator," *Vehicular Technology, IEEE Transactions on*, vol. 56, no. 6, pp. 3371–3380, Nov 2007.

[7] A. Amini, R. Vaghefi, J. de la Garza, and R. Buehrer, "Improving gps-based vehicle positioning for intelligent transportation systems," in *Intelligent Vehicles Symposium Proceedings, 2014 IEEE*, June 2014, pp. 1023–1029.

[8] D. Yang, F. Zhao, K. Liu, H. B. Lim, E. Frazzoli, and D. Rus, "A gps pseudorange based cooperative vehicular distance measurement technique," in *Vehicular Technology Conference (VTC Spring), 2012 IEEE 75th*, May 2012, pp. 1–5.

[9] F. Zhang, H. Stahle, G. Chen, C. Buckl, and A. Knoll, "Multiple vehicle cooperative localization under random finite set framework," in *2013 IEEE/RSJ International Conference on Intelligent Robots and Systems, Tokyo, Japan, November 3-7, 2013*, 2013, pp. 1405–1411.

[10] H. Wymeersch, J. Lien, and M. Win, "Cooperative localization in wireless networks," *Proceedings of the IEEE*, vol. 97, no. 2, pp. 427–450, Feb 2009.

[11] M. Punithan and S.-W. Seo, "King's graph-based neighbor-vehicle mapping framework," *Intelligent Transportation Systems, IEEE Transactions on*, vol. 14, no. 3, pp. 1313–1330, Sept 2013.

[12] Research and I. T. Administration. (2012) Vehicle-to-vehicle (V2V) communications for safety. http://www.its.dot.gov/research/v2v.htm.

[13] T. Rappaport, *Wireless Communications: Principles and Practice*, 2nd ed. Upper Saddle River, NJ, USA: Prentice Hall PTR, 2001.

[14] A. Goldsmith, *Wireless Communications*. Stanford University, 2004. [Online]. Available: http://www.cs.ucdavis.edu/ liu/289I/Material/book-goldsmith.pdf

[15] J. V. Stoep, "Design and implementation of reliable localization algorithms using received signal strength," Master's thesis, University of Washington, Washington US, 2009.

[16] P. Pathirana, N. Bulusu, A. Savkin, and S. Jha, "Node localization using mobile robots in delay-tolerant sensor networks," *Mobile Computing, IEEE Transactions on*, vol. 4, no. 3, pp. 285–296, May 2005.

[17] R. Miucic and S. Bai, "Performance of aftermarket (DSRC) antennas inside a passenger vehicle," *SAE International Journal of Passenger Cars - Electronic and Electrical Systems*, vol. 4, no. 1, pp. 150 – 155, 2011.

[18] P. Groves, *Principles of GNSS, Inertial, and Multisensor Integrated Navigation Systems, Second Edition:*, ser. GNSS/GPS. Artech House, 2013.